Revealing the role of Si vacancy and interface in $SiHCl_3$ dissociation applied in polysilicon

Mao Peng[a,b,d,#], Jia Ren[c,#], Wei Li[a], Chenliang Ye[e,*], Jinli Zhang[a,*]

[a] School of Chemical Engineering and Technology, Tianjin University, Tianjin 300350, China.

[b] Zhejiang Institute of Tianjin University, Shaoxing, 312300.

[c] Chinese Acad Sci, Shenzhen Inst Adv Technol, Adv Energy Storage Technol Res Ctr, Shenzhen 518055, China.

[d] State Key Laboratory of Silicon and Advanced Semiconductor Materials, Zhejiang University Hangzhou 310027, China.

[e] Department of Power Engineering, North China Electric Power University, Baoding 071003, Hebei, China.

* Corresponding author:

Jinli Zhang, *E-mail address*: zhangjinli@tju.edu.cn

Chenliang Ye, E-mail: chenliangye@ncepu.edu.cn

[#] These authors contributed equally to this work.

2 Calculational details

2.1 Selected models

To deeply explore the influence of Si vacancy and interface on $SiHCl_3$ reduction mechanism, we constructed the models in Figure 1 based on our previous studies [1]. Si(111)-V was formed based on perfect Si(111) surface with a Si vacancy, and the *p*(3×3) super cell was selects; the bottom one slab atoms were frozen, and the top two atomic layers with the adsorbed molecules were relaxed during optimization. Aiming at examining the effect of interface on $SiHCl_3$ reduction, three typical structure models was built based on previous investigation [2, 3]. Si_8/Si(111) interface were formed through placing Si_8 clusters on perfect *p*(4×4) super cell Si(111) surface; the bottom one slab atoms were frozen; the top two atomic layers, Si_8 cluster and adsorbed molecules were relaxed. Si_8/Si(111)-V1 and Si_8/Si(111)-V2 models showed that two different Si vacancies were formed on Si(111), and the distances between interface and Si vacancy were 2.573 and 4.361 Å, respectively. The vacuum degree of four models in *z* direction was set to 15 Å to avoid mutual interference.

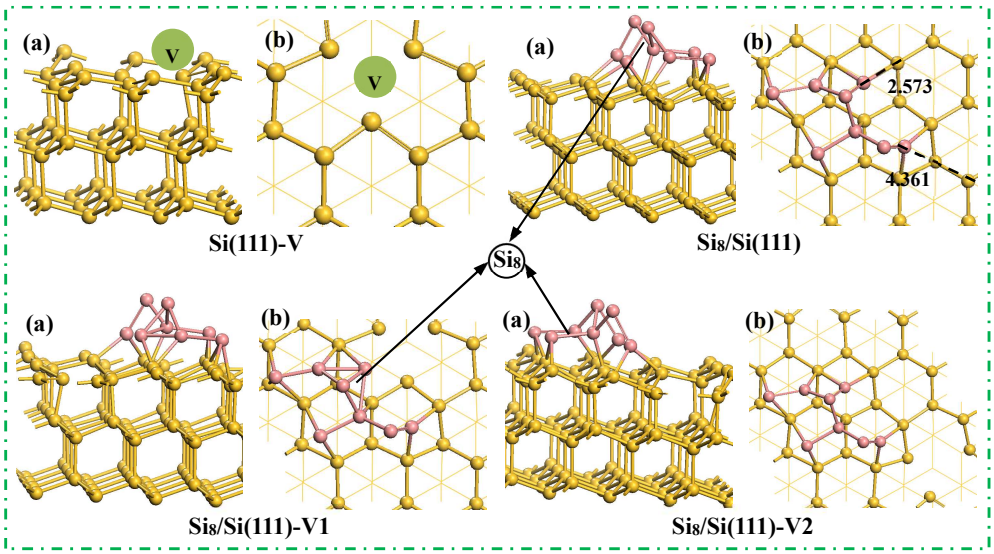

Figure S1. (a) side view and (b) top view of Si(111)-V, Si_8/Si(111), Si_8/Si(111)-V1 and Si_8/Si(111)-V2, respectively.

2.2 calculational methods

All calculation data were obtained using VASP software with PAW, and the exchange-correlation functional was performed by PBE pseudopotentials [4, 5]. Spin-polarization was included in all structures presented here. Si(111)-V adopted 3×3×1 Monkhorst–Pack k-point; the 2×2×1 k-point was performed for Si_8/Si(111), Si_8/Si(111)-V1 and Si_8/Si(111)-V2. We selected the cutoff energy of 400 eV and set the convergence accuracy of the force as 0.03 eV $Å^{-1}$. When the total energy change between two steps was both less than 1×10^{-5} eV, the electronic degree of freedom was converged. The transition states of all elementary reactions were calculated using the CI-NEB [6, 7] and dimer method [8, 9].

The activation free energy (ΔG_a) and reaction free energy (ΔG) are calculated according to the following

formula:

$$\Delta G_{\mathrm{a}} = E_{\mathrm{TS}} - E_{\mathrm{R}} + G_{\mathrm{TS}} - G_{\mathrm{R}} \tag{1}$$

$$\Delta G = E_{\mathrm{P}} - E_{\mathrm{R}} + G_{\mathrm{P}} - G_{\mathrm{R}} \tag{2}$$

where E_{R}, E_{TS} and E_{P} correspond to the total energies of reaction, transition state and production, respectively. G_{R}, G_{TS} and G_{p} are the Gibbs free energies of reaction, transition state and production at a finite temperature. The temperature was set as 1425 K based on the practical temperature range (1273~1623 K) [10, 11].

Reaction rate constant (k) can be obtained using harmonic Transition State Theory (TST) according to the Eq. (1)

$$k = \frac{k_B T}{h} \frac{q_{Ts}}{q_{Is}} exp\left(-\frac{Ea}{RT}\right) \tag{3}$$

Here Ea is the zero-point-corrected energy difference between the transition state and the initial state. For surface reactions, only the vibrational degrees of freedom have been considered for the partition functions (q), which is calculated in the harmonic model according to the Eq. (4).

$$q = \frac{-b \pm \sqrt{b^2 - 4ac}}{\prod_{i=1}^{Vibrations} 1 - \exp\left(\frac{-hv_i}{k_B T}\right) 2a} \tag{4}$$

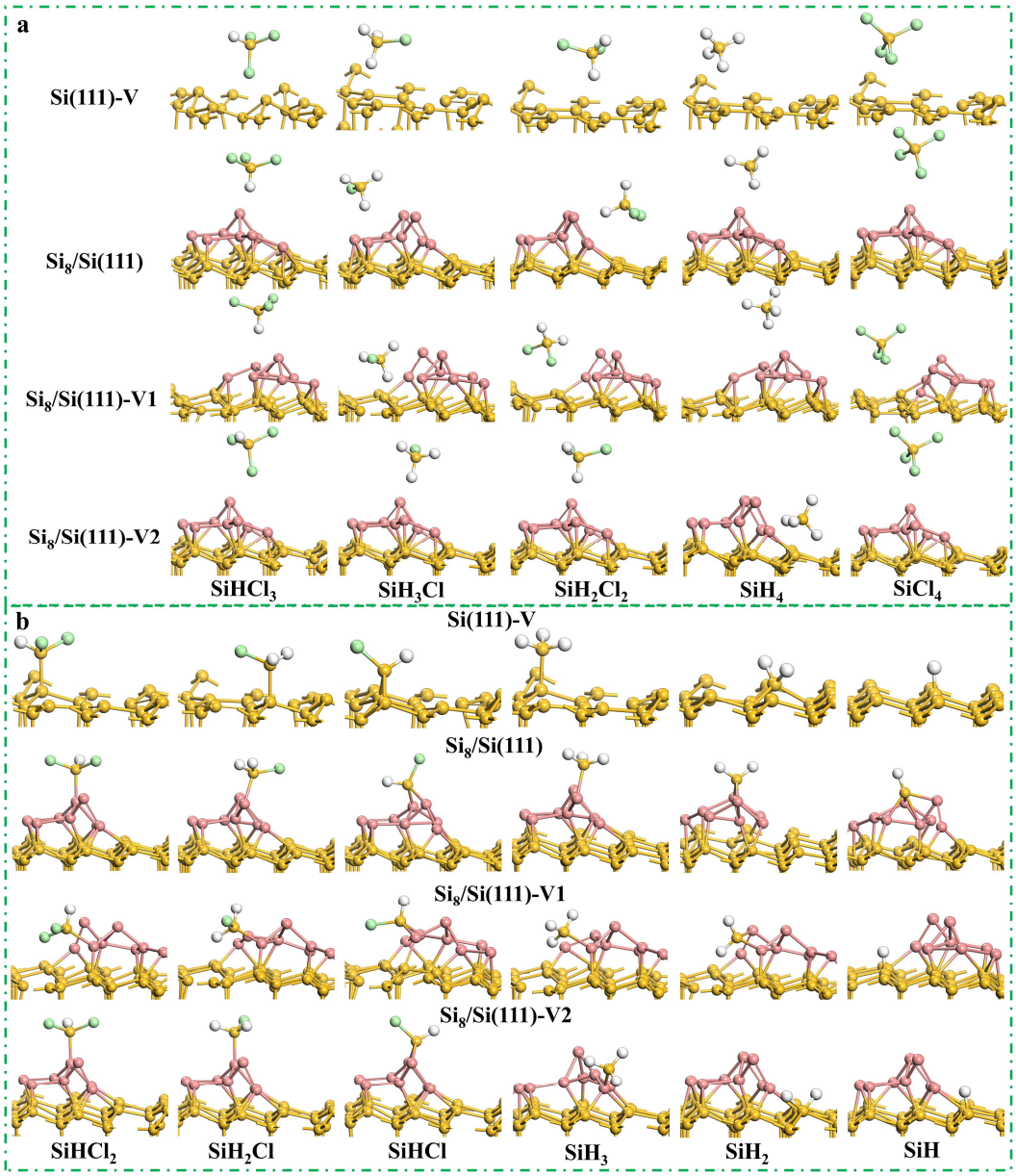

Figure S2. (a) The adsorption configurations of $SiHCl_3$, SiH_3Cl, SiH_2Cl_2, SiH_4 and $SiCl_4$ on Si(111)-V, Si_8/Si(111), Si_8/Si(111)-V1 and Si_8/Si(111)-V2 surfaces. (b) The most stable adsorption configurations of $SiHCl_2$, SiH_2Cl, SiHCl, SiH_3, SiH_2 and SiH on Si(111)-V, Si_8/Si(111), Si_8/Si(111)-V1 and Si_8/Si(111)-V2 surfaces. The Cl, Si and H atoms are shown in the green, yellow and white balls, respectively

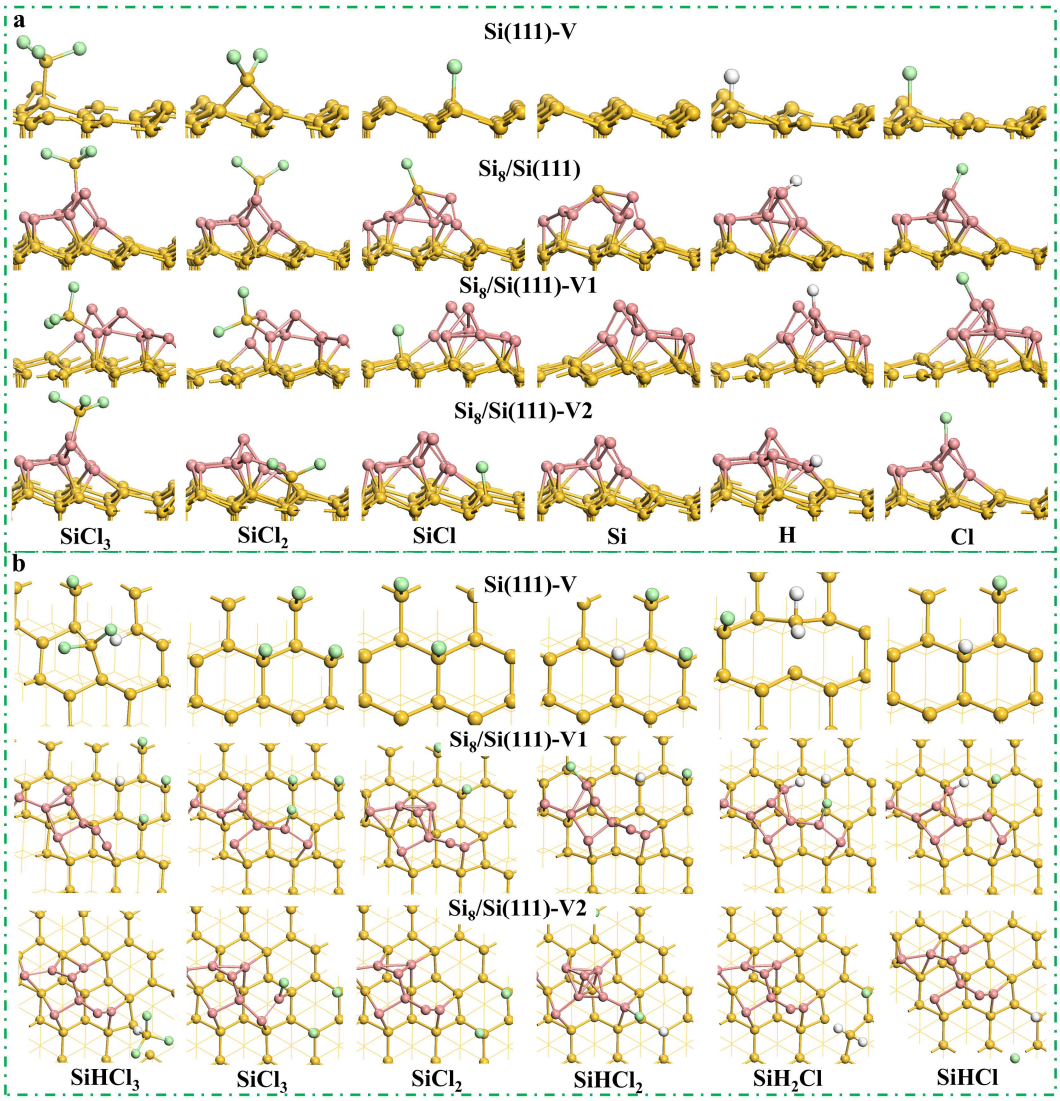

Figure S3. (a) The most stable adsorption configurations of $SiCl_3$, $SiCl_2$, SiCl, Si, H and Cl on Si(111)-V, Si_8/Si(111), Si_8/Si(111)-V1 and Si_8/Si(111)-V2 surfaces. (b) The adsorption configurations of $SiHCl_3$, $SiCl_3$, $SiCl_2$, $SiHCl_2$, SiH_2Cl and SiHCl on Si vacancy of Si(111)-V, Si_8/Si(111)-V1 and Si_8/Si(111)-V2 surfaces.

Table S1. The activation energies ($\triangle G_a$/kJ mol^{-1}) and reaction energies ($\triangle G$/kJ mol^{-1}) of each elementary reactions about $SiHCl_3$ reduction on Si (111)-V, Si_8/Si (111), Si_8/Si (111)-V1 and Si_8/Si (111)-V2 surfaces at 1425 K.

Elementary reactions	Si (111)-V		Si_8/Si (111)		Si_8/Si (111)-V1		Si_8/Si (111)-V2	
	$\triangle G_a$	$\triangle G$	$\triangle G_a$	$\triangle G$	$\triangle G_a$	$\triangle G$	$\triangle G_a$	$\triangle G$
$SiHCl_3 \rightarrow SiCl_3+H$	22.3	-190.0	173.9	24.3	151.3	17.1	83.9	-70.8
$SiHCl_3 \rightarrow SiHCl_2+Cl$	115.5	-218.6	128.5	26.7	122.6	51.0	108.8	-45.3
$SiCl_3 \rightarrow SiCl_2+Cl$	69.7	-72.5	97.5	-77.6	50.1	-41.5	88.5	16.4
$SiCl_3+Cl \rightarrow SiCl_4$	222.3	153.5	77.6	17.1	207.9	34.7	90.4	10.1
$SiHCl_2+H \rightarrow SiH_2Cl_2$	202.4	170.9	126.9	44.3	199.6	178.8	131.8	19.3
$SiHCl_2 \rightarrow SiHCl+Cl$	77.5	-48.5	85.5	-73.6	56.6	-61.1	55.6	-44.1
$SiHCl_2 \rightarrow SiCl_2+H$	45.1	-106.6	75.7	-88.1	105.6	-48.3	48.1	-51.7
$SiCl_2 \rightarrow SiCl+Cl$	62.4	-107.2	60.3	-143.7	74.3	44.3	27.5	-258.6
$SiHCl+H \rightarrow SiH_2Cl$	115.2	60.8	147.9	31.5	37.2	-57.7	141.1	38.0
$SiHCl \rightarrow SiCl+H$	71.6	-42.5	69.5	-104.4	106.0	-93.3	56.6	-106.9
$SiHCl \rightarrow SiH+Cl$	53.0	-101.7	121.3	-102.3	121.2	-36.0	59.2	-74.4
$SiH_2Cl+Cl \rightarrow SiH_2Cl_2$	224.4	165.4	155.1	117.4	209.9	156.5	79.1	7.2
$SiH_2Cl+H \rightarrow SiH_3Cl$	220.1	144.3	190.0	134.9	338.1	168.5	130.5	-8.6
$SiH_2Cl \rightarrow SiH_2+Cl$	56.1	-92.9	98.8	-56.4	41.5	-71.2	27.7	-85.1
$SiCl \rightarrow Si+Cl$	152.4	-0.4	136.8	-2.1	94.1	-14.1	41.8	-125.8
$SiH_2+H \rightarrow SiH_3$	157.4	29.8	68.9	42.0	98.0	97.6	43.6	-92.9
$SiH+H \rightarrow SiH_2$	268.4	228.0	54.3	19.6	69.6	15.5	264.9	221.7
$SiH_3+Cl \rightarrow SiH_3Cl$	247.7	182.2	237.3	120.7	202.5	201.9	81.4	-23.5
$SiH_3+H \rightarrow SiH_4$	208.4	119.4	130.5	-3.1	95.4	38.7	274.9	221.4
$SiH \rightarrow Si+H$	159.1	-6.1	44.0	-13.3	87.4	-28.8	29.4	-29.6

Table S2. The rate constants k (s^{-1}) of each elementary reactions involved in $SiHCl_3$ reduction on Si (111)-V, Si_8/Si (111), Si_8/Si (111)-V1 and Si_8/Si (111)-V2 surfaces at 1425 K.

Elementary reactions	Si (111)-V	Si_8/Si (111)	Si_8/Si (111)-V1	Si_8/Si (111)-V2
$SiHCl_3 \rightarrow SiCl_3+H$	4.52×10^{12}	1.25×10^{7}	8.44×10^{7}	2.50×10^{10}
$SiHCl_3 \rightarrow SiHCl_2+Cl$	1.72×10^{9}	5.75×10^{8}	9.48×10^{8}	3.05×10^{9}
$SiCl_3 \rightarrow SiCl_2+Cl$	8.27×10^{10}	7.92×10^{9}	8.67×10^{11}	1.69×10^{10}
$SiCl_3+Cl \rightarrow SiCl_4$	2.10×10^{5}	4.23×10^{10}	7.05×10^{5}	1.44×10^{10}
$SiHCl_2+H \rightarrow SiH_2Cl_2$	1.12×10^{6}	6.59×10^{8}	1.42×10^{6}	4.39×10^{8}
$SiHCl_2 \rightarrow SiHCl+Cl$	4.27×10^{10}	2.17×10^{10}	2.50×10^{11}	2.71×10^{11}
$SiHCl_2 \rightarrow SiCl_2+H$	6.61×10^{11}	4.96×10^{10}	4.00×10^{9}	5.11×10^{11}
$SiCl_2 \rightarrow SiCl+Cl$	1.53×10^{11}	1.83×10^{11}	5.62×10^{10}	2.91×10^{12}
$SiHCl+H \rightarrow SiH_2Cl$	1.77×10^{9}	1.12×10^{8}	1.29×10^{12}	2.00×10^{8}
$SiHCl \rightarrow SiCl+H$	7.01×10^{10}	8.44×10^{10}	3.86×10^{9}	2.51×10^{11}
$SiHCl \rightarrow SiH+Cl$	3.37×10^{11}	1.06×10^{9}	1.07×10^{9}	2.01×10^{11}
$SiH_2Cl+Cl \rightarrow SiH_2Cl_2$	1.76×10^{5}	6.09×10^{7}	5.99×10^{5}	3.74×10^{10}
$SiH_2Cl+H \rightarrow SiH_3Cl$	2.52×10^{5}	3.22×10^{6}	1.19×10	4.89×10^{8}
$SiH_2Cl \rightarrow SiH_2+Cl$	2.60×10^{11}	7.08×10^{9}	8.93×10^{11}	2.86×10^{12}
$SiCl \rightarrow Si+Cl$	7.65×10^{7}	2.87×10^{8}	1.06×10^{10}	8.69×10^{11}
$SH_2+H \rightarrow SiH_3$	5.05×10^{7}	8.86×10^{10}	7.61×10^{9}	7.50×10^{11}
$SiH+H \rightarrow SiH_2$	4.26×10^{3}	3.03×10^{11}	8.32×10^{10}	5.75×10^{3}
$SiH_3+Cl \rightarrow SiH_3Cl$	2.46×10^{4}	5.93×10^{4}	1.12×10^{6}	3.07×10^{10}
$SiH_3+H \rightarrow SiH_4$	6.78×10^{5}	4.87×10^{8}	9.44×10^{9}	2.46×10^{3}
$SiH \rightarrow Si+H$	4.37×10^{7}	7.21×10^{11}	1.86×10^{10}	2.49×10^{12}

Table S3. The only one imaginary frequency corresponding to the transition states involved in reduction mechanism on Si(111)-V, Si_8/Si(111), Si_8/Si(111)-V1 and Si_8/Si(111)-V2

Elementary reactions	Frequency/cm^{-1}			
	Si(111)-V	Si_8/Si(111)	Si_8/Si(111)-V1	Si_8/Si(111)-V2
$SiHCl_3 \rightarrow SiCl_3+H$	179	134	94	119
$SiHCl_3 \rightarrow SiHCl_2+Cl$	204	83	93	133
$SiCl_3+Cl \rightarrow SiCl_4$	58	109	148	109
$SiCl_3 \rightarrow SiCl_2+Cl$	145	83	92	185
$SiCl_2 \rightarrow SiCl+Cl$	68	131	100	62
$SiCl \rightarrow Si+Cl$	83	126	94	131
$SiHCl_2 \rightarrow SiCl_2+H$	46	129	185	97
$SiHCl_2 \rightarrow SiHCl+Cl$	41	146	95	87
$SiHCl_2+H \rightarrow SiH_2Cl_2$	349	237	93	214
$SiHCl \rightarrow SiCl+H$	653	283	211	470
$SiHCl \rightarrow SiH+Cl$	105	119	43	70
$SiH \rightarrow Si+H$	1050	972	576	250
$SiHCl+H \rightarrow SiH_2Cl$	166	354	180	198
$SiH_2Cl+Cl \rightarrow SiH_2Cl_2$	183	261	160	141
$SiH_2Cl+H \rightarrow SiH_3Cl$	142	349	296	275
$SiH_2Cl \rightarrow SiH_2+Cl$	137	227	150	131
$SiH+H \rightarrow SiH_2$	200	329	285	602
$SiH_2+H \rightarrow SiH_3$	459	693	436	224
$SiH_3+H \rightarrow SiH_4$	204	419	165	105
$SiH_3+Cl \rightarrow SiH_3Cl$	552	256	379	91

1. M. Peng, B. Z. Shi, Y. Han, W. Li and J. L. Zhang, *Applied Surface Science*, 2022, **580**.
2. J. L. Gong and X. H. Bao, *Chemical Society Reviews*, 2017, **46**, 1770-1771.
3. J. A. Rodriguez, D. C. Grinter, Z. Y. Liu, R. M. Palomino and S. D. Senanayake, *Chemical Society Reviews*, 2017, **46**, 1824-1841.
4. P. Honenberg and W. Kohn, *Resonance-Journal of Science Education*, 2017, **22**, 810-811.
5. J. P. Perdew, K. Burke and M. Ernzerhof, *Physical Review Letters*, 1996, **77**, 3865-3868.
6. D. Sheppard, P. H. Xiao, W. Chemelewski, D. D. Johnson and G. Henkelman, *Journal of Chemical Physics*, 2012, **136**.
7. D. Sheppard, R. Terrell and G. Henkelman, *Journal of Chemical Physics*, 2008, **128**.
8. G. Henkelman and H. Jónsson, *Journal of Chemical Physics*, 1999, **111**, 7010-7022.
9. R. A. Olsen, G. J. Kroes, G. Henkelman, A. Arnaldsson and H. Jónsson, *Journal of Chemical Physics*, 2004, **121**, 9776-9792.
10. T. A. Halgren and W. N. Lipscomb, *Chemical Physics Letters*, 1977, **49**, 225-232.
11. K. Yasuda, K. Saegusa and T. H. Okabe, *Materials Transactions*, 2009, **50**, 2873-2878.